



Diel bio-optical variability observed from moored sensors in the Arabian Sea

C.S. Kinkade^{a,*}, J. Marra^b, T.D. Dickey^c, C. Langdon^b,
D.E. Sigurdson^c, R. Weller^d

^a*Department of Earth and Environmental Sciences, Lamont-Doherty Earth Observatory of Columbia University, Palisades, NY 10964, USA*

^b*Lamont-Doherty Earth Observatory of Columbia University, Palisades, NY 10964, USA*

^c*ICESS, UC Santa Barbara, CA 93106, USA*

^d*Woods Hole Oceanographic Institution, Woods Hole, MA 02543, USA*

Received 7 September 1997; received in revised form 13 July 1998; accepted 20 July 1998

Abstract

As part of the Forced Upper Ocean Dynamics Program, which ran concurrently with the US JGOFS Arabian Sea Expedition, five moorings were deployed in the historical axis of the Findlater Jet. In addition to other variables, moored sensors collected photosynthetically active radiation (PAR), particulate beam attenuation (C_p), stimulated fluorescence (FLU), and dissolved oxygen (O_2) data from October 1994 to October 1995. Diel bio-optical signals were recorded during two periods between the Northeast and Southwest Monsoons at 10, 35, and 65 m. Spectral analysis shows significant diel cycles of C_p , FLU, and O_2 , but the strength of these cycles was not constant over time. Daily periodicity was lowest for all bio-optical signals just after a strong storm during the 1994 Fall Intermonsoon period. During a phytoplankton bloom associated with a cool advective feature, the FLU and O_2 diel signals were most pronounced. Although these signals are biological responses to the daily cycle of irradiance, they are mediated by hydrographic conditions; strongest when phytoplankton are confined within the mixed layer or thermocline, and thus exposed to light intensities long enough to display these responses to PAR. Fluorescence quenching at 10 m due to high irradiance ($\sim 1000 \mu\text{Einstein m}^{-2} \text{s}^{-1}$) forced the ratio of fluorescence to particulate attenuation into a diel periodicity at 10 m, but not at 35 m (noon irradiance $\sim 200 \mu\text{Einstein m}^{-2} \text{s}^{-1}$), where the FLU and C_p increases were almost in phase. Diel changes in C_p , when scaled to particulate organic carbon, suggest a net production of $\sim 20 \text{ mg C m}^{-3} \text{ d}^{-1}$ at 10 and 35 m. We estimate a specific growth rate from a calculated particle production rate balanced by

* Corresponding author. Fax: 001-619-594-8670.

E-mail address: csk@chors.sdsu.edu (C.S. Kinkade)

¹ Present address: Center for Hydro-Optics and Remote Sensing, San Diego, CA 92120, USA.

a constant grazing over 24 h to be 0.77 d^{-1} , and using a C_c^* of 424 mg C m^{-2} , estimate a carbon : chl *a* ratio between 85 and 115 for a 10-d window during the 1994 Fall Intermonsoon period. © 1999 Elsevier Science Ltd. All rights reserved.

1. Introduction

Changes in open-ocean optical properties are largely caused by changes in the suspended particulate matter, and key contributor to these changes are the phytoplankton. Phytoplankton physiological processes operate on time scales of tens of seconds to hours, with the diel time scale on the order of the generation time of individual algal cells, making the diel irradiance cycle an important source of variability.

There has been extensive research on diel variations in phytoplankton properties, including changes in biomass, photosynthetic parameters and rates, cell division, chlorophyll fluorescence, cellular pigment changes, nutrient assimilation, and beam attenuation (see Prézélin (1992), Stramska and Dickey (1992a) and Marra (1997) for literature reviews). With the exception of some recent studies (e.g., LeBouteillier and Herbland, 1982; Siegel et al., 1989; Gardner et al., 1993,1995,1999; Durand and Olson, 1996), most shipboard sampling programs have not sampled frequently enough to characterize the daily cycle of phytoplankton in the open ocean. Also, these studies have focused on diel changes in either fluorescence or particulate attenuation, but not both. Because of a high sampling frequency, moored sensors have provided excellent platforms to study diel variability in multiple bio-optical properties (Dickey, 1991; Marra, 1994,1997; Dickey et al., 1998). The extent and significance of diel signals in bio-optical properties have been reported from near-surface drifters as well as the Biowatt and the Marine-Light Mixed Layers moorings (Hamilton et al., 1990; Dickey et al., 1991; Stramska and Dickey, 1992b; Abbott et al., 1995; Marra, 1997).

Concurrent with the US Joint Global Ocean Flux Study (US JGOFS) Arabian Sea Expedition, five hydrographic and atmospheric moorings were deployed in the central Arabian Sea (15.5° N , 61.5° E) for two six-month deployments from 15 October 1994 to 20 October 1995 as part of the ONR sponsored Forced Upper Ocean Dynamics Program. A general overview of data from the five moorings is presented in Rudnick et al. (1997), and the meteorological conditions and atmospheric forcing can be found in Weller et al. (1998). The central mooring was the most heavily instrumented; the hydrographic and bio-optical conditions and central mooring schematic can be found in Dickey et al. (1998). Marra et al. (1998) model primary productivity from bio-optical sensors on the central mooring. Here we present bio-optical data from the central mooring focusing on variability on the diel time scale.

2. Methods

Multi-variable moored systems (MVMS) were deployed at 10, 35, 65 and 80 m depth on the central surface mooring (see Dickey et al. (1989,1998), Ho et al. (1996a,b),

Sigurdson et al. (1995,1996) for details including discussion of sensor calibration). The MVMS package measures photosynthetically active radiation (PAR), natural and stimulated fluorescence, beam transmission at 660 nm (C), dissolved oxygen, orthogonal horizontal currents, temperature and conductivity. Data presented here are 15-min averages. Although the mooring was deployed during the 1994 Fall Intermonsoon, all data are referenced to 1995 yeardays; seasonal definitions are Fall Intermonsoon, mooring deployment 14 October 1994 to 31 October 1994 (yeardays – 77 to – 61); Northeast Monsoon, 1 November 1994 to 15 February 1995 (yeardays – 60 to 46); Spring Intermonsoon, 16 February 1995 to 31 May 1995 (yeardays 47–151) and Southwest Monsoon, 1 June 1995 to 15 September 1995 (yeardays 152–258).

The data returns from the moorings were good, considering the 6-month optical instrument deployments in productive tropical waters, but bio-fouling was significant at times (specifics and timelines of sensor functionality are given in Ho et al. (1996a,b) and Sigurdson et al. (1995,1996). For the present report, we used times when PAR, fluorescence, particulate attenuation and dissolved oxygen sensors were all operational at 10 and 35 m, with the exception of the 35 m fluorometer and PAR sensor late in the Spring Intermonsoon. These times were during the Fall Intermonsoon and early NE Monsoon, 14 October – 20 November (yeardays – 77 to – 40) and the Spring Intermonsoon/early SW Monsoon, 1 April – 10 May (yeardays 120 – 160).

The coefficient of beam attenuation is the sum of absorption and scattering contributions from pure water (C_w), yellow substance (C_y), and particles (C_p):

$$C = C_w + C_y + C_p.$$

C_w is widely held to be a constant, and, in the open ocean at 660 nm, C_y is assumed negligible (Jerlov, 1976), so variations in the attenuation from suspended particles, C_p , primarily determine variations in C . By convention, fluorometers are calibrated with chlorophyll a ; here fluorescence is reported in units of chlorophyll, mg m^{-3} . Mixed-layer depth (MLD) was calculated as a 0.125 kg m^{-3} difference in density from the surface water. Even with 27 temperature sensors deployed in the upper 100 m, the steep temperature gradient at the base of the mixed layer causes the calculated MLD to get “pinned” to a sensor depth by the linear interpolation between two sensors. Despite this effect producing a mixed-layer depth “baseline”, the diel signal is still evident.

2.1. Bio-optical coherences with PAR

Following spectral analysis methods of Kay (1988) and Bloomfield (1976), we used the estimated squared coherence statistic to compare pairs of time series. The squared coherence is calculated by

$$\text{coherence}^2 = \frac{|P_{12}(f)|^2}{P_{11}(f)P_{22}(f)},$$

where $P_{12}(f)$ is the cross spectral density of signals 1 and 2, $P_{11}(f)$ is the power spectrum density of signal 1, and $P_{22}(f)$ is the power spectrum density of signal 2. The

coherence is essentially a correlation coefficient of the power spectra of two time series, which shows the degree of correlation as a function of frequency. The squared coherence values range from zero (no correlation at a given frequency) to one (perfect correlation). We calculated the C_p , FLU and O_2 signals' coherence with PAR to get the correlation with (or strength of) the diel signal. A higher coherence value with PAR at the diel frequency (1 cpd) indicates a stronger diel periodicity. Because the time-series were nonstationary, we detrended the data by removing the means, using a 5-d window. Following Stramska and Dickey (1992a) to estimate the variation in squared coherence over time, we calculated the coherence at the diel frequency for 10-d windows of the detrended time series, and plotted the value as the first day in the series (i.e., the calculated squared coherence for data from days 120–129 is plotted as day 120).

2.2. Productivity, specific growth rate and *C:chl a* estimates from beam attenuation

Because beam attenuation has been shown to be highly correlated with suspended particle mass and particulate organic carbon (POC), diel changes in particulate beam attenuation (ΔC_p) have been used to estimate primary productivity (Siegel et al., 1989; Cullen et al., 1992a; Cullen and Lewis, 1995; Gardner et al., 1995; Walsh et al., 1995). A crucial assumption is the conversion factor from particulate attenuation to POC, the carbon specific beam attenuation coefficient, C_c^* . The seasonal range of C_c^* measured during the US JGOFS Arabian Sea expedition over an annual cycle was 387–508 mg C m⁻² (Gundersen et al., 1998). We use a value of 424 mg C m⁻², calculated by regression of shipboard C_p (from cruise TN043) on POC for the only profile near the mooring during the Northeast Monsoon ($n = 20$, $r^2 = 0.97$) (I. Gundersen, pers. comm and US JGOFS database: <http://jgofswww.whoi.edu>). Thus, the diel change in C_p was multiplied by a C_c^* of 424 mg C m⁻² to estimate phytoplankton carbon assimilation.

Cullen et al. (1992a) showed that converting ΔC_p to estimates of photosynthesis also specifies the growth rate of the phytoplankton, μ (d⁻¹), (w:w). We followed the reasoning of Siegel et al. (1989) and Cullen et al. (1992a), estimating specific particle production rate, r , from the diel change in attenuation:

$$r = \frac{1}{t} \ln \left(\frac{C_{\max}}{C_{\min}} \right),$$

where t is the time between daily minimum and maximum beam attenuation. We estimated a specific growth rate from a 24-h balance of particle production and a constant grazing (g); $r = \mu - g$. To calculate a carbon : chl *a* ratio, an assumption must be made about the proportion that phytoplankton contributes to the POC, because absolute C_p values are used (not ΔC_p as in estimating carbon assimilation above). In the Equatorial Pacific Ocean, Eppley et al. (1992) measured autotrophs to be 30% of POC, while Cullen and Lewis (1995) used 50%. In the northeastern Atlantic Ocean, Marra et al. (1995) used transmissometer and fluorometer data to estimate 65–85% phytoplankton contribution to POC. Dennett et al. (1999) measured

nano- and microplankton biomass to be 25–35% of the POC in the top 160 m during the 1995 Northeast Monsoon. For lack of direct measurement near the mooring, we adopt a value of 50%, and calculate a carbon : chl *a* ratio from C_p , the C_c^* and the fluorometer estimate of chlorophyll *a*.

3. Results

Fig. 1a and b show the PAR, C_p , FLU, and O_2 signals at 10 m as well as the MLD for the Fall Intermonsoon/early Northeast Monsoon and Spring Intermonsoon/early Southwest Monsoon. Records of PAR, C_p and FLU at 35 m are presented in Fig. 2a and b for the same time periods. A strong storm at the beginning of the Fall

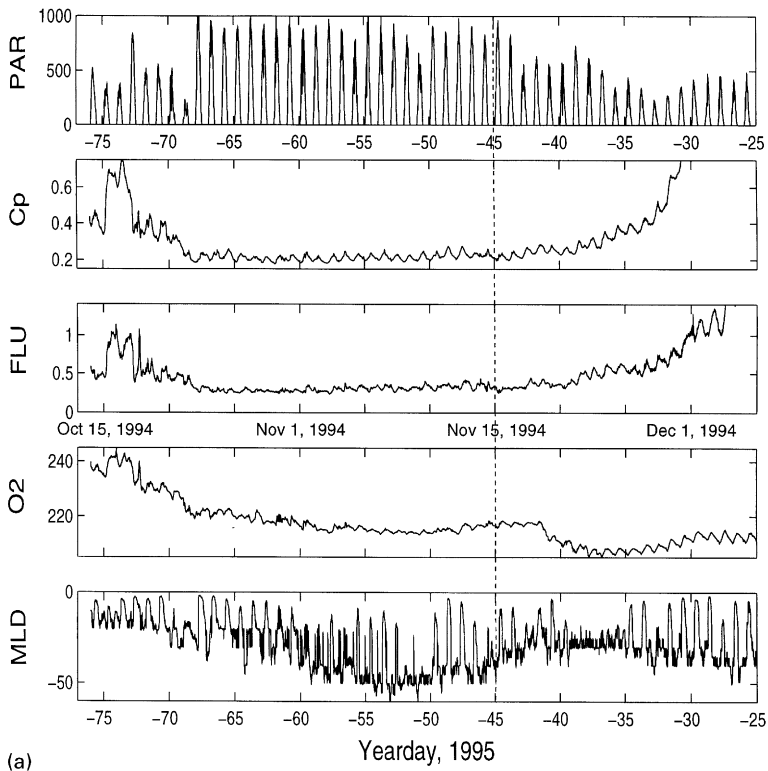


Fig. 1. Time series from the 10 m MVMS from (a) the Fall Intermonsoon period, 1995 yeardays – 77 to – 40; and (b) the Spring Intermonsoon period, 1995 yeardays 120–160. Plotted from top to bottom, photosynthetically available radiation (PAR; $\mu\text{Einstein m}^{-2} \text{s}^{-1}$), particulate beam attenuation (C_p ; m^{-1}), stimulated fluorescence (FLU; $\mu\text{g chl l}^{-1}$), dissolved oxygen (O_2 ; μmol), and mixed layer depth (MLD; $10.125 \sigma_t$; m). Vertical dotted line in (a) marks the start of an advective feature passing by the mooring (see text).

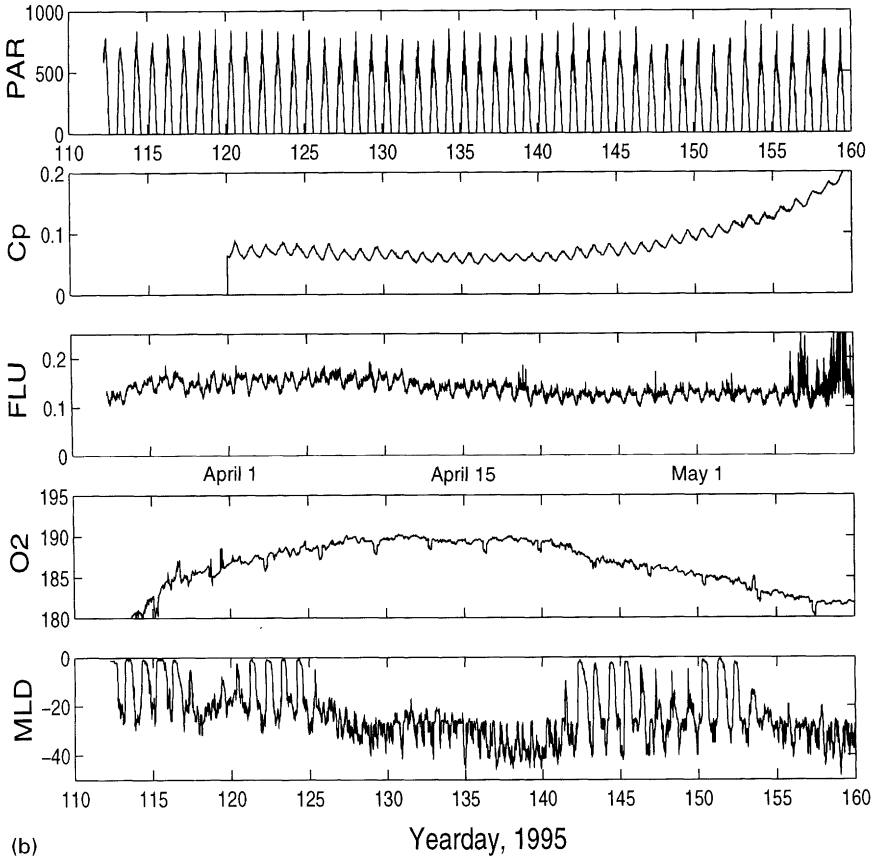


Fig. 1. (Continued)

Intermonsoon record is marked by decreased PAR, increased C_p , FLU, and O_2 . After that event, there are clear diel signals that persist until the sensors became fouled with the onset of the NE Monsoon. During the Spring Intermonsoon, there was no easily discernible diel signal in the 10 m O_2 , but the other signals show a diel pattern again until bio-fouling near the beginning of the SW Monsoon.

A mesoscale advective feature passed the mooring site during yeardays - 45 to - 20 (Sigurdson, 1996), marked by shifting current direction and shoaling isotherms (see Fig. 5, Dickey et al., 1998). The cold feature was evident in the 10 m bio-optical signals as increased FLU and C_p , decreased O_2 , and increased diel change in C_p , FLU and O_2 . There is also a dampening of the daily MLD excursion from day - 40 to - 35.

The daily C_p signal is quite evident at 10 and 35 m, but minimal at 65 m (Fig. 3), with a higher frequency variation; temperature records show internal waves moving past the 65 m MVMS. The 10 m C_p has a minimum at dawn, and a maximum near

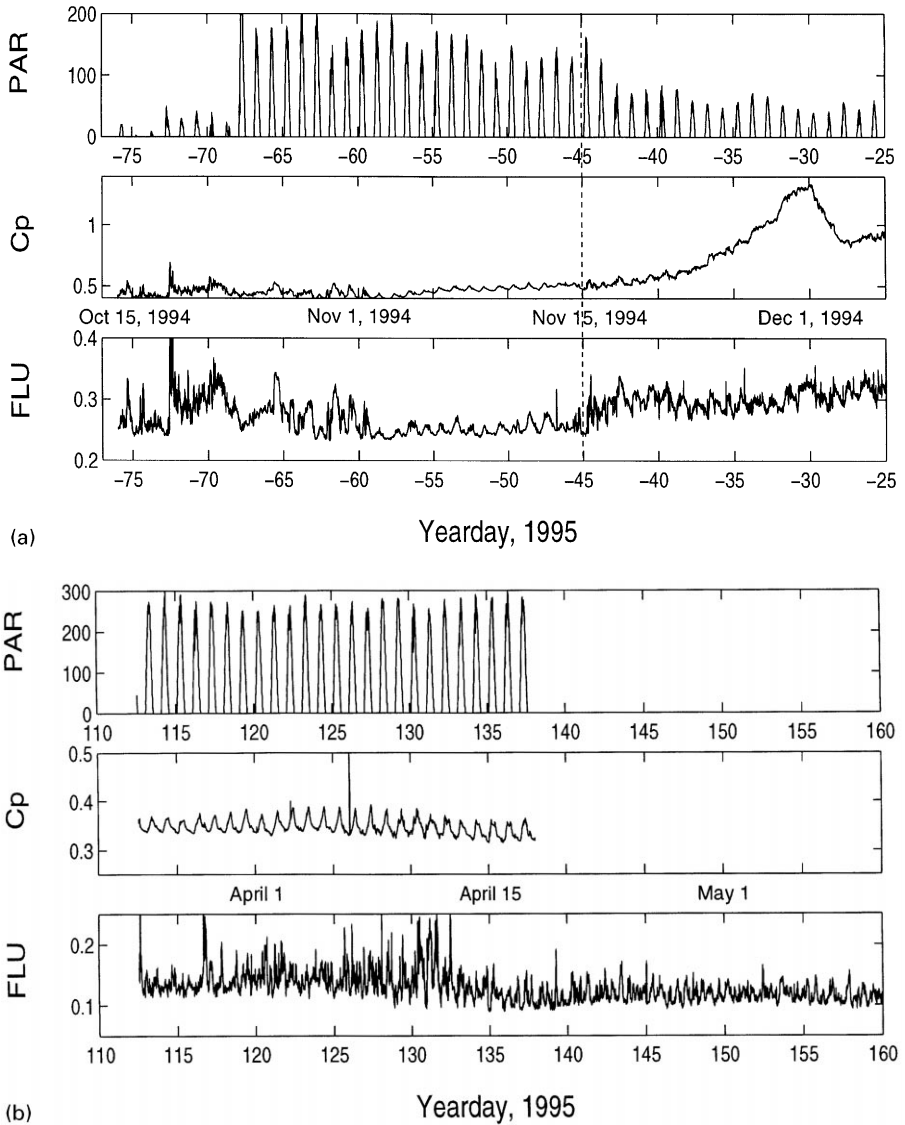


Fig. 2. Time series from the 35 m MVMS; top to bottom, PAR ($\mu\text{Einstein m}^{-2} \text{s}^{-1}$), C_p (m^{-1}), FLU ($\mu\text{g chl l}^{-1}$) for the Fall Intermonsoon (a) and Spring Intermonsoon (b). Vertical dotted line in (a) marks the start of an advective feature passing by the mooring (see text).

sunset each day (Fig. 4a). This is consistent with several previous high-frequency observations (e.g., Siegel et al., 1989; Stramska and Dickey, 1992b). The FLU time series shows a local minimum at noon each day, as well as a fast response to short-term variations in PAR due to clouds (e.g., yearday -55, Fig. 4a). The 35 m

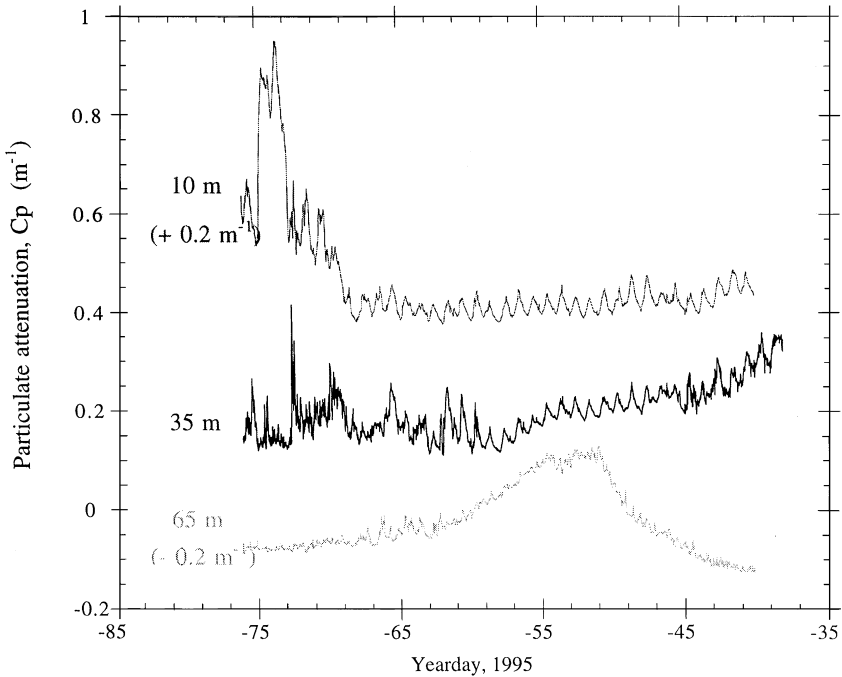


Fig. 3. Particulate beam attenuation at 10, 35 and 65 m. The 10 m signal is offset by $+0.2 \text{ m}^{-1}$ and 65 m is offset by -0.2 m^{-1} to avoid overlap.

C_p (Fig. 4b) has a minimum at dawn, but a maximum before sunset, while the 35 m FLU is almost in phase with C_p . It is possible that diel changes in the MLD, the timing of cell division, and zooplankton grazing are affecting the particulate signal earlier in the day at 35 m than at 10 m. The role of diel variations in MLD on carbon assimilation and export in the Arabian Sea is discussed in Gardner et al. (1999).

3.1. Bio-optical coherences with PAR

During the Fall Intermonsoon, the coherence spectrum of PAR- C_p and PAR- O_2 at 10 m show significant peaks at the diurnal or diel (1 cpd) and semi-diurnal (2 cpd) frequencies (Fig. 5a), while the PAR-FLU coherence was not as high at the diel frequency. The Spring Intermonsoon 10 m coherence spectrum (Fig. 5b) shows PAR- C_p and PAR-FLU diel peaks high and broader than during the Fall Intermonsoon, but the O_2 coherence was not significant at the diel frequency.

Fig. 6 shows how the statistical significance of the diel periodicity of C_p , FLU, O_2 and MLD changes during the Fall Intermonsoon. Also shown on these plots is the temperature difference between the surface and 35 m (dotted line) for hydrographic reference. The C_p diel signal (Fig. 6a) is weak at the beginning of the record after the

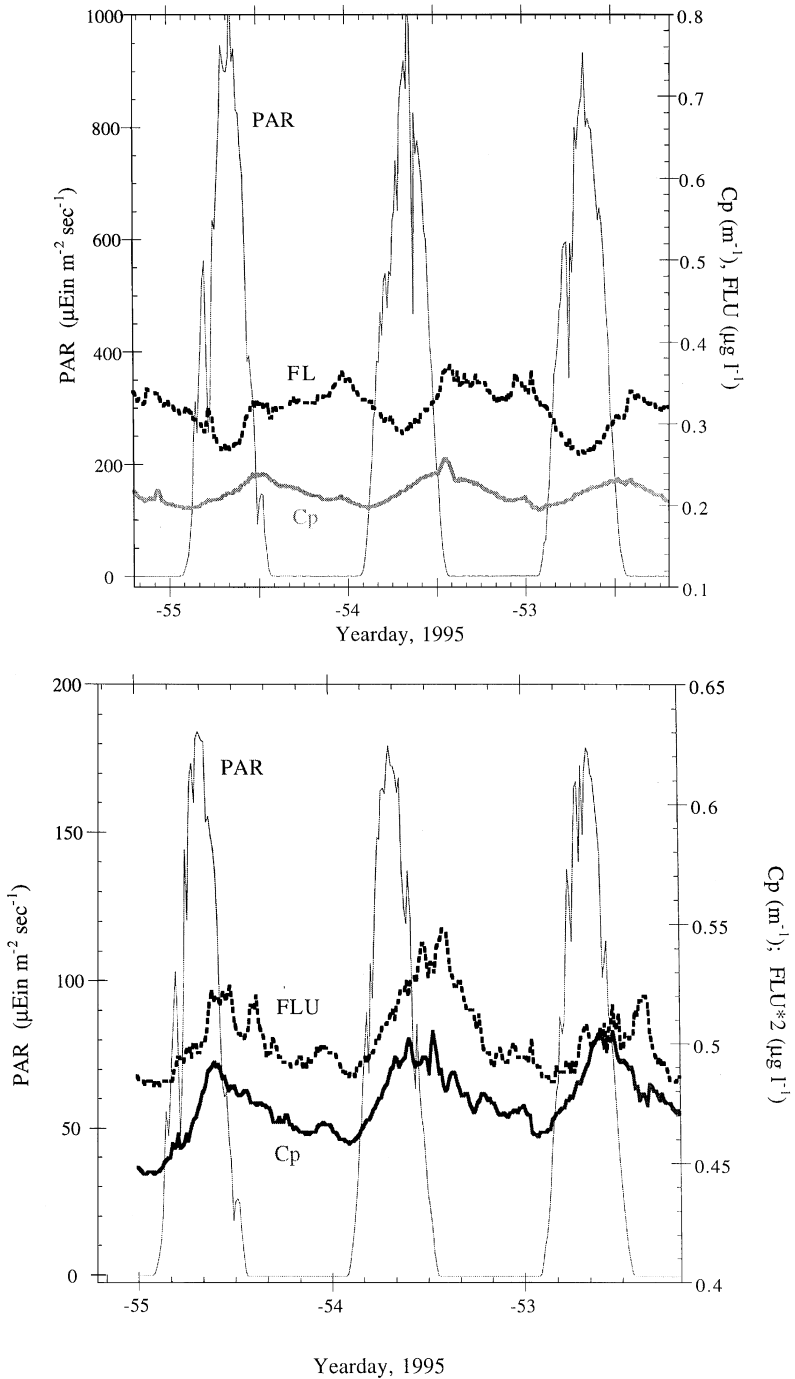


Fig. 4. PAR, C_p and FLU over three days during the Fall Intermonsoon; (a) 10 m, (b) 35 m.

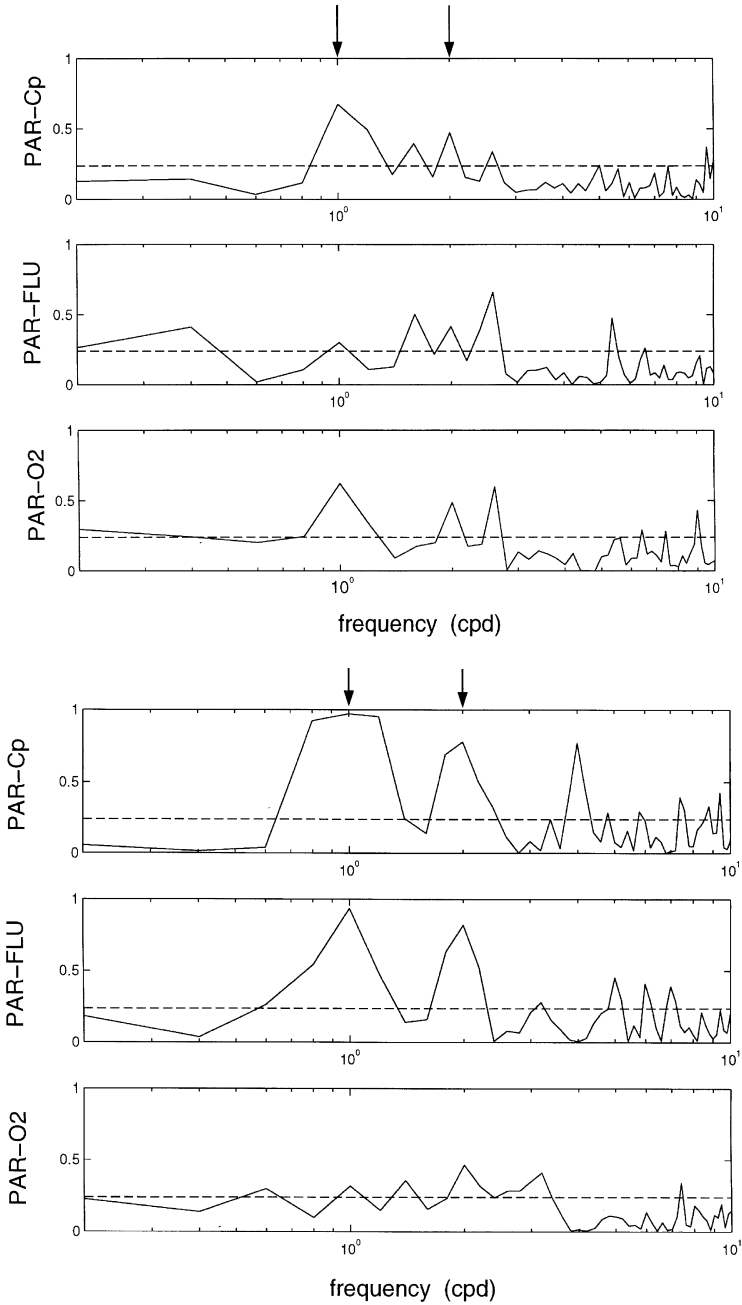


Fig. 5. Estimated squared coherence spectra of PAR and C_p , PAR and FLU, and PAR and O_2 during (a) the Fall Intermonsoon, yeardays -77 to -40, and (b) the Spring Intermonsoon, yeardays 120–160. Arrows indicate peaks at 1 and 2 cycles per day; the diel or diurnal and semi-diurnal signal. Dotted lines are the cutoff values for a peak to be significantly different from zero.

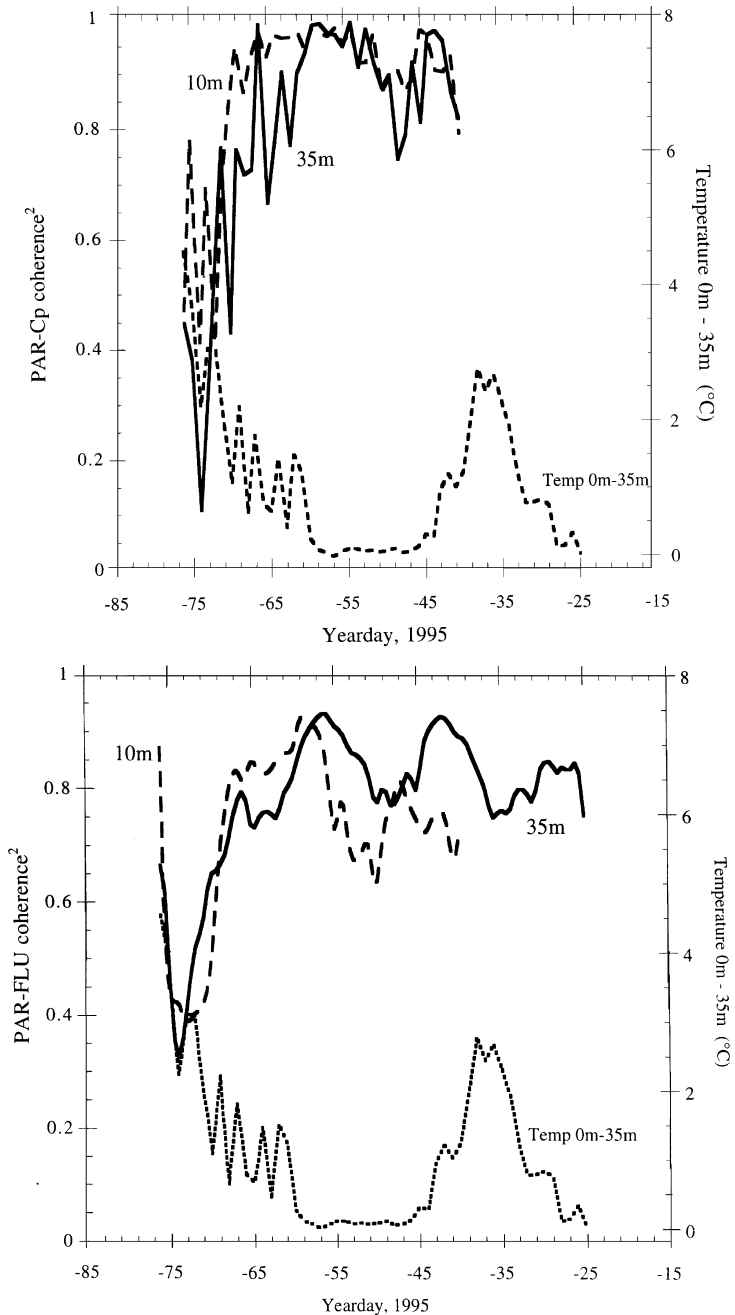


Fig. 6. Time series of (a) PAR- C_p and (b) PAR-FLU estimated squared coherences at the diel frequency at 10 and 35 m during the first deployment (solid lines). (c) Estimated squared coherence time series for 10 m PAR- O_2 . (d) Estimated squared coherence time series for 10 m PAR-MLD. Dashed lines are temperature difference between 0 m (measured from the surface buoy) and 35 m.

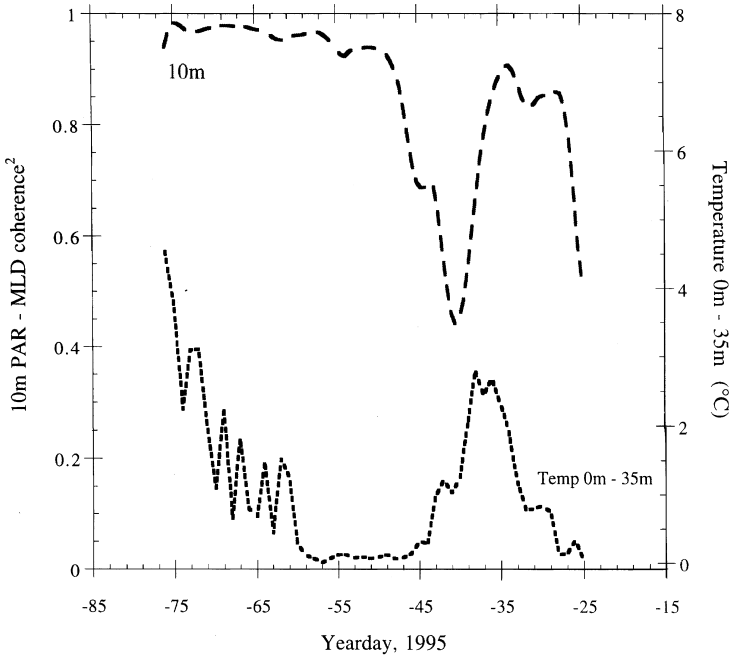
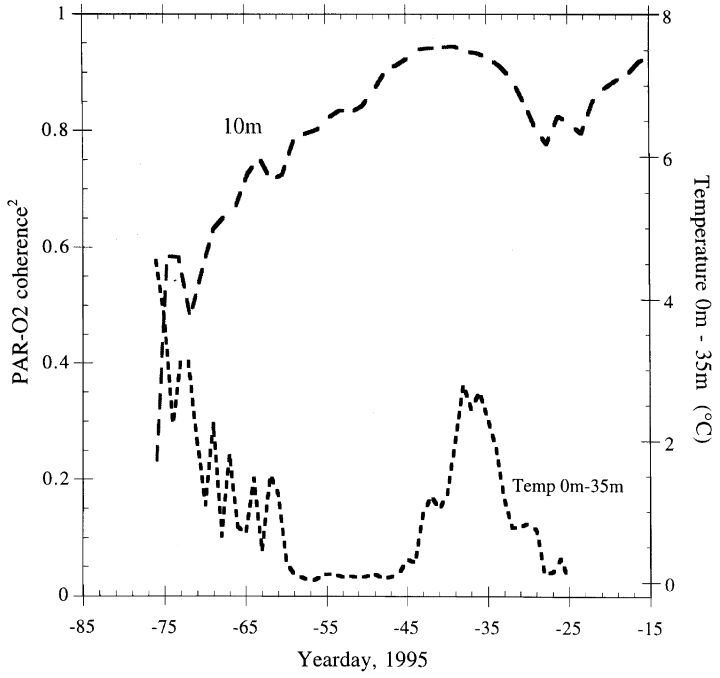


Fig. 6. (Continued)

wind-mixing event, then strengthens and stays highly coherent with PAR into the advective event until around yearday -35 , when biofouling is most likely affecting the signal. The FLU diel signal (Fig. 6b) is also weaker after the storm, but stays highly significant through the time when the eddy is passing. The O_2 daily signal periodicity (Fig. 6c) is similar to the C_p and FLU time series, weakly diel at the start, then intensifying and most pronounced during the advective event. The MLD diel signal (Fig. 6d) is strong until the MLD excursions are dampened during the beginning of the cool advective feature; the drop, however, is not concurrent with the low C_p diel periodicity.

3.2. Productivity, specific growth rate and C : chl a estimates from beam attenuation

For the 10 d window between wind mixing and advective events during the Fall Intermonsoon (yeardays -55 to -46), we estimate an average specific particle production rate of 0.045 h^{-1} . Balanced by a 24 h grazing, this gives a maximum specific growth rate of 0.77 d^{-1} . Using the measured C_c^* of 424 mg C m^{-2} to scale the changes in particulate attenuation to carbon, we calculate an average carbon uptake of 21.2 and $19.5 \text{ mg C m}^{-3} \text{ d}^{-1}$ at 10 and 35 m, respectively. The phytoplankton POC and fluorometer chlorophyll a values produce an estimate of phytoplankton carbon: chl a ratio varying between 85 at dawn and 115 at dusk at 35 m.

4. Discussion

4.1. Bio-optical coherences with PAR

On the shelf edge in the Mid-Atlantic Bight, Flagg et al. (1994) found low coherences between ADCP current measurements and phytoplankton biomass measured from moored fluorometers, as well as low acoustic zooplankton measurements and phytoplankton biomass coherence. They attributed the low coherences to the competing influences of local biological processes, spatial variability, vertical shear and zooplankton migrations. Our bio-optical time series of C_p , FLU, and O_2 , as well as the coherences with PAR are affected by a balance between physiological and physical processes (advection and mixing), as well as production and grazing.

When the mixed layer shoals during the passage of the mesoscale eddy, the C_p daily cycle weakens, but the FLU and O_2 diel amplitudes remain pronounced. Changes in fluorescence and biological oxygen evolution take place rapidly, on the time scale of tens of seconds to hours (Marra and Heinemann, 1982; Cullen et al., 1988; Stramska and Dickey, 1992a). C_p , however, integrates the response to PAR over a longer time scale, not as a function of short-term changes in irradiance.

The C_p diel signal is strongest when the phytoplankton concentrations are greatest in the mixed layer. As the mixed layer shoals during the advective event, individual algal cells are exposed to higher average light intensity, allowing growth. The O_2 diel signal is stronger, net O_2 production rises, and there is an increase in FLU and C_p as phytoplankton biomass accumulates. Higher C_p and O_2 diel periodicity has been

reported with the onset of the spring bloom in the North Atlantic (Stramska and Dickey, 1992b). Here we have shown a stronger diel signal in O_2 during a bloom due to an advective event.

4.2. FLU/C_p ratio

Fluorescence is a loss of radiative energy, which would otherwise be converted to chemical energy or heat. Under the relatively high irradiance at 10 m (5 fold higher than at 35 m, 1000 vs. $\sim 200 \mu\text{Einstein m}^{-2} \text{s}^{-1}$) the quantum efficiency of fluorescence decreases due to a competitive interaction between the loss of excitation energy through fluorescence and nonphotochemical quenching processes (e.g., xanthophyll cycles and reaction center quenching). (Demmig-Adams, 1990; Demers et al., 1991; Kiefer and Reynolds, 1992; Long et al., 1994)

As mentioned above, C_p and FLU change on different time scales, the physiological FLU signal being faster, so relating FLU to C_p has been used in the literature to study photoadaptive processes (Denman and Gargett, 1988; Cullen et al., 1992a; Stramska and Dickey, 1992b). Fig. 7 shows (from top to bottom) PAR at 10 m, the ratio of FLU to C_p at 10 m, PAR at 35 m and FLU/C_p at 35 m for 3 d during the Fall Intermonsoon. At 10 m, this ratio undergoes large diel changes as FLU drops in response to the high irradiance as C_p rises with particle production. The 35 m ratio has no easily discerned diel signal; C_p and FLU are nearly in phase and there is little fluorescence quenching at the lower light intensities deeper in the water column. This diel pattern of FLU/C_p at 10 m can be seen in a plot of FLU/C_p as a difference from dawn against PAR for 5 d during the Fall Intermonsoon (Fig. 8). Just after dawn, there is possibly a shouldering of FLU/C_p and then a sharp decline as particles are produced in the water column and fluorescence quenching starts. After solar noon, with declining irradiance, the FLU/C_p increases again, but with a different slope. The dark period is required for complete recovery of the FLU and thus the FLU/C_p ratio to the dawn value. The pattern of PAR-induced depression of fluorescence has been noted in moored fluorometers (Marra, 1992), shipboard fluorescence profiles (Cullen and Lewis, 1995), laboratory cultures (Cullen et al., 1988), and near-surface drifters (Abbott et al., 1990).

4.3. Productivity, specific growth rate and C :chl *a* estimates from beam attenuation

Scaling C_p to community phytoplankton carbon concentrations, carbon assimilation and growth rates makes the assumption that there is a constant conversion from particulate attenuation to phytoplankton carbon, C_c^* . The value measured by Siegel et al. (1989) and adopted by Cullen et al. (1992a) was 255 mg C m^{-2} , the range measured in the Arabian Sea 387–508 (Gundersen et al., 1998). The constancy of C_c^* has been discussed by Cullen and Lewis (1995) and investigated in recent laboratory studies (Olson et al., 1990; Ackleson et al., 1990, 1993; Stramski and Reynolds, 1995; Stramski et al., 1995); there has been some evidence for carbon-independent changes in C_c^* , although not necessarily with a diel periodicity. Without spatially or temporally relevant independent measurements for comparison, we used a simple

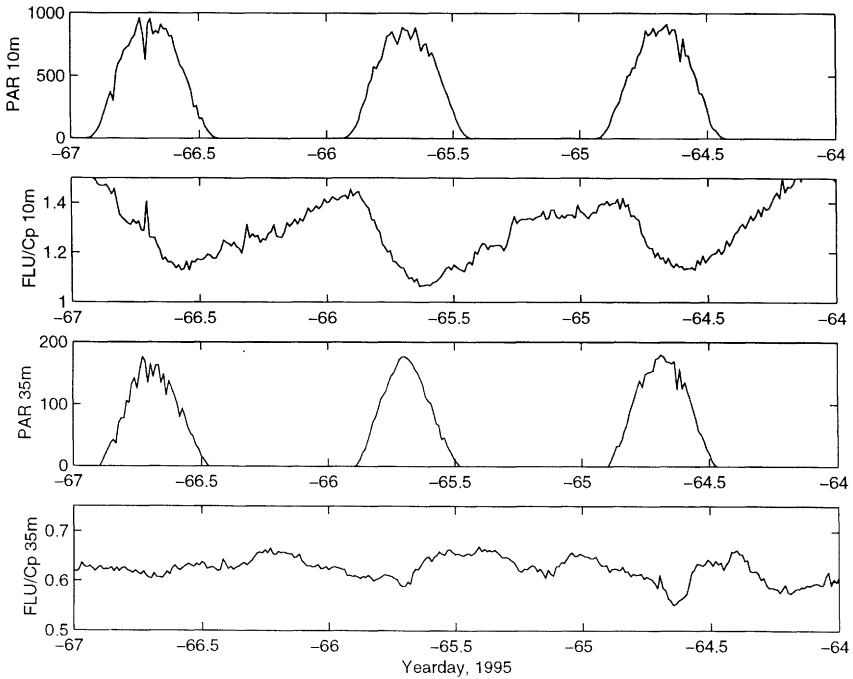


Fig. 7. From top to bottom, 10 m PAR ($\mu\text{Einstein m}^{-2} \text{s}^{-1}$), 10 m FLU/ C_p ratio ($\mu\text{g l}^{-1} \text{m}^{-1}$), 35 m PAR, 35 m FLU/ C_p .

optical model for productivity and growth rate. Our growth rate estimate of 0.77 d^{-1} and carbon : chl *a* estimate of 85–115 is lower than the $\mu = 1.2 \text{ d}^{-1}$ and up to a factor of 2.5 higher than the average carbon : chl *a* of 44 measured during the Northeast Monsoon (cruise TN043; R. Goericke and JGOFS database). Admittedly, ignoring changes in C_c^* or diel variability in grazing (Siegel et al., 1989) are oversimplifications. Cullen and Lewis (1995), using a C_c^* of 500 mg C m^{-2} with a daily variation of 30% in a physiological–optical model, were able to reconcile growth rates and carbon uptake estimated by particle dynamics with independent measurements in the Equatorial Pacific Ocean.

Although there were no productivity measurements at this time near the mooring, we can make a comparison with the carbon assimilation model of Marra et al. (1998). They modeled primary productivity using surface irradiance and moored fluorescence data with an assumed quantum efficiency, and an independently estimated phytoplankton absorption coefficient. For yeardays -55 to -46 , Marra et al. (1998) estimate $27.7 \text{ mg C m}^{-3} \text{ d}^{-1}$ at 10 m, and $6.2 \text{ mg C m}^{-3} \text{ d}^{-1}$ at 35 m, compared with our particle-derived estimates of 21.2 and $19.5 \text{ mg C m}^{-3} \text{ d}^{-1}$ at 10 and 35 m. While differences in the estimates are difficult to assess, there are several differences in the approaches of the two models. The Marra et al. model uses solar irradiance as a key parameter, which decreases with depth as a function of the diffuse attenuation

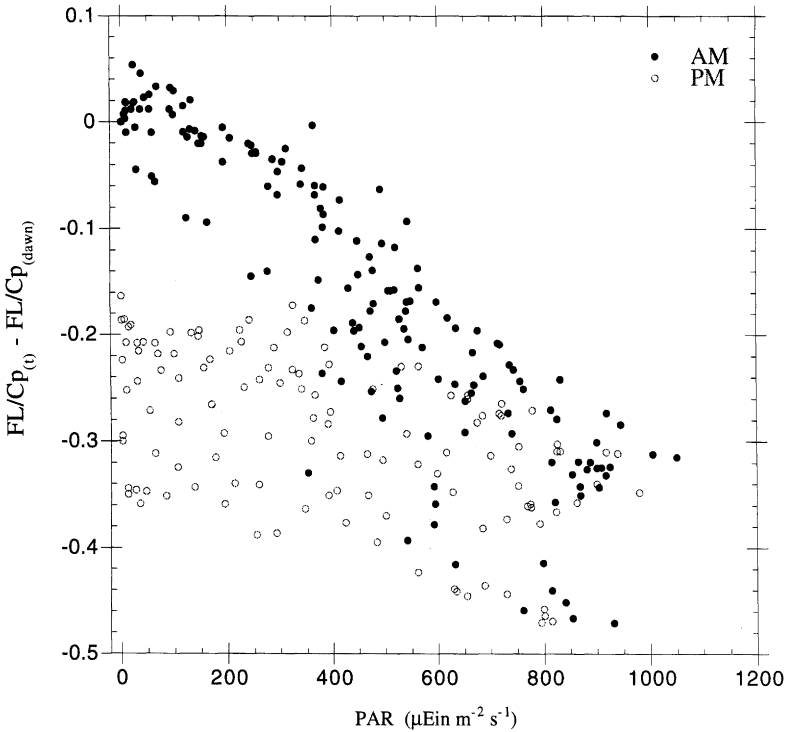


Fig. 8. FL/Cp_p ratio plotted as the difference from the dawn value against PAR for year days – 55 to – 51. Closed circles are data before local noon and open circles are data collected after local noon.

coefficient, while the two sensors for the particle estimate of carbon assimilation were both in the mixed layer for the entire period. This may explain the relatively depth-constant particle estimate of carbon uptake versus the irradiance–fluorescence model. Also, the irradiance–fluorescence model is tuned to incubated bottle ^{14}C samples, which measure something between net and gross carbon uptake, while the particulate estimate should be measuring net production, without bottle effects. Additionally, the incubated ^{14}C samples are from the JGOFS standard station S07, since there was no productivity data available from the mooring site, so spatial heterogeneity would be expected to add to the discrepancy. Finally, the ^{14}C incubations are taken from times other than the 10-d window chosen here (see Marra et al., 1998, Fig. 2d).

We have shown strong diel periodicity in particulate attenuation, stimulated fluorescence and dissolved oxygen in the Arabian Sea, although the strength of these signals was not constant over time. The changes in the strength of diel bio-optical signals are largely driven by changes in the water column (e.g., MLD and stratification), not by changes in irradiance. Although these signals are biological responses to the daily cycle of irradiance, they are mediated by hydrographic conditions; strongest

when phytoplankton are trapped within the mixed layer or stratified water that exposes them to irradiances long enough to display these responses to PAR.

Acknowledgements

This work was supported by the Office of Naval Research grant # N00014-94-1-0450 and N00014-96-1-0505. The manuscript was greatly improved by the comments and suggestions of John Cullen and two anonymous reviewers. This is US JGOFS contribution number 434.

References

- Abbott, M.R., Brink, K.H., Booth, C.R., Blasco, D., Codispoti, L.A., Niiler, P.P., Ramp, S.R., 1990. Observations of phytoplankton and nutrients from a lagrangian drifter off northern California. *Journal of Geophysical Research* 95, 9393–9409.
- Abbott, M.R., Brink, K.H., Booth, C.R., Blasco, D., Swenson, M., Davis, C.O., Codispoti, L.A., 1995. Scales of variability of bio-optical properties as observed from near-surface drifters. *Journal of Geophysical Research* 100, 13,345–13,367.
- Ackleson, S.G., Cullen, J.J., Brown, J., Lesser, M., 1990. Some changes in the optical properties of marine phytoplankton in response to high light intensity. *SPIE: Ocean Optics X* 1302, 238–249.
- Ackleson, S.G., Cullen, J.J., Brown, J., Lesser, M.P., 1993. Irradiance-induced variability in light scatter from marine phytoplankton in culture. *Journal of Plankton Research* 15, 737–759.
- Bloomfield, P., 1976. *Fourier Analysis of Time Series: An Introduction*. Wiley, New York, pp. 258.
- Cullen, J.J., Lewis, M.R., 1995. Biological processes and optical measurements near the sea surface: Some issues relevant to remote sensing. *Journal of Geophysical Research* 100, 13,255–13,266.
- Cullen, J.J., Lewis, M.R., Davis, C.O., Barber, R.T., 1992a. Photosynthetic characteristics and estimated growth rates indicate grazing is the proximate control of primary production in the equatorial pacific. *Journal of Geophysical Research* 97, 639–654.
- Cullen, J.J., Yentsch, C.S., Cucci, T.L., MacIntyre, H.L., 1988. Autofluorescence and other optical properties as tools in biological oceanography. *SPIE: Ocean Optics IX* 925, 149–156.
- Demers, S., Roy, S., Gagnon, R., Vignault, C., 1991. Rapid light-induced changes in cell fluorescence and in xanthophyll-cycle pigments of *Alexandrium excavatum* (Dinophyceae) and *Thalassiosira pseudonana* (Bacillariophyceae): a photo-protection mechanism. *Marine Ecology Progress Series* 76, 185–193.
- Demmig-Adams, B., 1990. Carotenoids and photoprotection in plants: a role for the xanthophyll zeaxanthin. *Biochemica et Biophysica Acta* 1020, 1–24.
- Denman, K.L., Gargett, A.E., 1988. Multiple thermoclines are barriers to vertical exchange in the subarctic Pacific during SUPER, May 1984. *Journal of Marine Research* 46, 77–103.
- Dennett, M.R., Caron, D.A., Murzov, S.A., Polikarpov, I.G., Gavrilova, N.A., Georgieva, L.V., Kuzmenko, L.V., 1999. Abundance and biomass of nano- and microplankton during the 1995 Northeast Monsoon and Spring Intermonsoon in the Arabian Sea. *Deep Sea Research II* 46, 1691–1717.
- Dickey, T.D., 1991. The emergence of concurrent high resolution physical and bio-optical measurements in the upper ocean and their application. *Review of Geophysics* 29, 383–413.
- Dickey, T.D., Marra, J., Sigurdson, D.E., Weller, R.A., Kinkade, C.S., Zedler, S.E., Wiggert, J.D., Langdon, C., 1998. Seasonal variability of bio-optical and physical properties in the Arabian Sea: October 1994–October 1995. *Deep Sea Research II* 45, 2001–2026.
- Dickey, T.D., Marra, J., Stramska, M., Langdon, C., Granata, T., Plueddemann, A., Weller, R., Yoder, J., 1989. Bio-optical and physical variability in the subarctic North Atlantic Ocean during the spring of 1989. *Journal of Geophysical Research* 99, 22,541–22,556.

- Durand, M.D., Olson, R.J., 1996. Contributions of light scattering and cell concentration changes to diel variations in beam attenuation in the equatorial Pacific from flow cytometric measurements of pico-, ultra- and nanoplankton. *Deep Sea Research II* 43, 891–906.
- Eppley, R.W., Chavez, F.P., Barber, R.T., 1992. Standing stocks of particulate carbon and nitrogen in the equatorial Pacific at 150°W. *Journal of Geophysical Research* 97, 655–662.
- Flagg, C.N., Wirick, C.D., Smith, S.L., 1994. The interaction of phytoplankton, zooplankton and currents from 15 months of continuous data in the Mid-Atlantic Bight. *Deep-Sea Research II* 41, 411–436.
- Gardner, W.D., Chung, S.P., Richardson, M.J., Walsh, I.D., 1995. The oceanic mixed-layer pump. *Deep-Sea Research II* 42, 757–775.
- Gardner, W.D., Gundersen, J.S., Richardson, M.J., Walsh, I.D., 1999. The role of seasonal and diel changes in mixed-layer depth carbon and chlorophyll distributions in the Arabian Sea. *Deep-Sea Research II* 46, 1833–1858.
- Gardner, W.D., Walsh, I.D., Richardson, M.J., 1993. Biophysical forcing of particle production and distribution during a spring bloom in the North Atlantic. *Deep-Sea Research II* 40, 171–195.
- Gundersen, J.S., Gardner, W.D., Richardson, M.J., Walsh, I.D., 1998. Effects of monsoons on the temporal and spatial variations of POC and chlorophyll in the Arabian Sea. *Deep Sea Research II* 45, 2103–2132.
- Hamilton, M.K., Granata, T.C., Dickey, T.D., Wiggert, J., Siegel, D.A., Marra, J., Langdon, C., 1990. Diel variations of bio-optical properties in the Sargasso Sea. *SPIE: Ocean Optics X* 1302, 214–224.
- Ho, C., Kinkade, C.S., Langdon, C., Maccio, M., Marra, J., 1996a. The Forced Upper Ocean Dynamics experiment in the Arabian Sea. Results from the multi-variable moored sensors from deployment-1 of the WHOI mooring. LDEO technical report LDEO-96-5, pp. 19 + figs.
- Ho, C., Kinkade, C.S., Langdon, C., Maccio, M., Marra, J., 1996b. The Forced Upper Ocean Dynamics experiment in the Arabian Sea. Results from the multi-variable moored sensors from deployment-2 of the WHOI mooring. LDEO technical report LDEO-96-8, pp. 19 + figs.
- Jerlov, N.G., 1976. *Marine Optics*. second ed. Elsevier Oceanography Series, vol. 14. Elsevier, Amsterdam, pp. 371.
- Kay, S.M., 1988. *Modern spectral estimation*. Prentice-Hall, Englewood Cliffs, N.J., pp. 454.
- Kiefer, D.A., Reynolds, R.A., 1992. Advances in understanding phytoplankton fluorescence and photosynthesis. In: Falkowski, P.G., Woodhead, A. (Eds.), *Primary Productivity and Biogeochemical Cycles in the Sea*. Plenum, New York, pp. 155–174.
- LeBouteillier, A., Herbland, A., 1982. Diel variation of chlorophyll *a* as evidenced from a 13-day station in the equatorial Atlantic Ocean. *Oceanologica Acta* 5, 433–441.
- Long, S.P., Humphries, S., Falkowski, P.G., 1994. Photoinhibition of photosynthesis in nature. *Annual Review of Plant Physiology and Plant Molecular Biology* 45, 633–662.
- Marra, J., 1992. Diurnal variability in chlorophyll fluorescence: observations and modeling. *Proceedings of the SPIE International Society of Optical Engineering* 1750, 233–244.
- Marra, J., 1994. Capabilities and merits of long-term bio-optical moorings. In: Spinrad, R., Perry, M., Carder, K., *Ocean Optics*, Oxford University Press, Oxford.
- Marra, J., 1997. Analysis of diel variability in chlorophyll fluorescence. *Journal of Marine Research* 55, 767–784.
- Marra, J., Dickey, T.D., Ho, C., Kinkade, C.S., Sigurdson, D., Weller, R., Barber, R.T., 1998. Variability in primary production as observed from moored sensors in the central Arabian Sea in 1995. *Deep Sea Research II* 45, 2253–2268.
- Marra, J., Heinemann, K., 1982. Photosynthesis response by phytoplankton to sunlight variability. *Limnology and Oceanography* 27, 1141–1152.
- Marra, J., Langdon, C., Knudson, C., 1995. Primary production, water column changes, and the demise of a *Phaeocystis* bloom at the Marine-Light Mixed Layers site (59°N, 21°W) in the northeast Atlantic Ocean. *Journal of Geophysical Research* 100, 6633–6643.
- Olson, R.J., Chisholm, S.W., Zettler, E.R., Armbrust, E.V., 1990. Pigments, size and distribution of *Synechococcus* in the North Atlantic and Pacific Oceans. *Limnology and Oceanography* 35, 45–58.
- Prézélin, B.B., 1992. Diel periodicity in phytoplankton productivity. *Hydrobiologia* 238, 1–35.

- Rudnick, D., Weller, R.A., Eriksen, C., Dickey, T.D., Marra, J., Langdon, C., 1997. One-year moored observations of the Arabian Sea Monsoons. *EOS* 78, 120–121.
- Siegel, D.A., Dickey, T.D., Washburn, L., Hamilton, M.K., Mitchell, B.G., 1989. Optical determination of particulate abundance and production variations in the oligotrophic ocean. *Deep Sea Research* 36, 211–222.
- Sigurdson, D.E., 1996. Analysis of physical and bio-optical variability in the Arabian Sea during the Northeast monsoon of 1994. M.S. Thesis, University of Southern California, pp. 124.
- Sigurdson, D.E., Dickey, T.D., Manov, D., 1995. Arabian Sea mooring data report: Deployment #1, October 15, 1994–April 20, 1995. Ocean Physics Laboratory Technical Report #OPL-2-95.
- Sigurdson, D.E., Dickey, T.D., Manov, D., 1996. Arabian Sea mooring data report: Deployment #2, April 22–October 20, 1995. Ocean Physics Laboratory Technical Report #OPL-2-96.
- Stramska, M., Dickey, T.D., 1992a. Short-term variations of the bio-optical properties of the ocean in response to cloud-induced irradiance fluctuations. *Journal of Geophysical Research* 97, 5713–5721.
- Stramska, M., Dickey, T.D., 1992b. Variability of bio-optical properties of the upper ocean associated with diel cycles in phytoplankton population. *Journal of Geophysical Research* 97, 17,813–17,887.
- Stramski, D., Shalapyonok, A., Reynolds, R.A., 1995. Optical characterization of the oceanic unicellular cyanobacterium *Synechococcus* grown under a day–night cycle in natural irradiance. *Journal of Geophysical Research* 100, 13,295–13,307.
- Walsh, I.D., Chung, S.P., Richardson, M.J., Gardner, W.D. 1995. The diel cycle in the Integrated Particle Load in the equatorial Pacific: A comparison with primary production, *Deep-Sea Research II* 42, 465–477.
- Weller, R.A., Baumgartner, M.F., Josey, S.A., Fischer, A.S., Kindle, J., 1998. Atmospheric forcing in the Arabian Sea during 1994–1995: observations and comparisons with climatology and models. *Deep Sea Research II* 45, 1961–2000.